Lattice and electronic structure properties of $\mathbf{GaAs_{1-x}P_x}$ semiconducting alloy

Lattice and electronic structure properties of GaAs$_{1-x}$P$_x$ semiconducting alloy

San-Guo Shen†‡ and Xi-Qing Fan‡

† China Center of Advanced Science and Technology (World Laboratory), PO Box 8730, Beijing,100080, People's Republic of China
‡ Physics and Engineering College, Zhengzhou University, Zhengzhou 450052, People's Republic of China

Abstract. Using a tight-binding bond orbital model, the local atomic structure of GaAs$_{1-x}$P$_x$ solid solution is calculated. The results are compared with theoretical results obtained by the valence force-field model calculation and experimental results obtained by extended x-ray absorption fine structure measurements and are found to be in good agreement with experiments. The calculated bond polarities, the bulk modulus, elastic constants, force constants, Young's modulus and sound velocities of GaAs and GaP are in good agreement with the existing experimental data. All of the results of GaAs$_{1-x}$P$_x$ alloys are predicated in the virtual crystal approximation. It is found that the bulk modulus, elastic constants, force constants, Young's modulus and sound velocities monotonically increase with increasing P composition and the increase is dominated by the change in average bond length. The electronic band structure of GaAs$_{1-x}$P$_x$ is obtained. The crossover composition $x_c = 0.43$. The results of the direct-band-gap energy are in very good agreement with the photoluminescence measurement data. The effective electron mass associated with the conduction band minimum in direct-band-gap GaAs$_{1-x}$P$_x$ alloy is estimated based on the $\boldsymbol{k} \cdot \boldsymbol{p}$ theory and is in good agreement with the optically detected cyclotron resonance and magnetoluminescence experimental results.

1. Introduction

GaAs$_x$P$_{1-x}$ alloy is one of the important semiconductor materials and is known to form solid solutions over the entire composition range. Its applications in light-emitting diodes and detectors are well known, and its physical properties have been investigated in great detail.

The atomic structure of the alloy is important in understanding its properties, in which the bond-length relaxation and the lattice constant are the key parameters. Theories of bond-length relaxation and the lattice constant in alloy have been given by Pauling and Vegard for a long time. Pauling [1] noted that the bond lengths in alloy are the sum of their constituent-element atomic radii, i.e., the bond lengths are independent of the alloy composition. Vegard [2] discovered that the lattice constant is approximately equal to the composition-weighted average of the lattice constants of the pure materials, i.e., the lattice constant is dependent on the alloy composition. The local structures of GaAs$_{1-x}$P$_x$ alloys have been determined by x-ray diffraction and extend x-ray absorption fine structure (EXAFS) experiments [3] recently, which have shown that the Ga–As and Ga–P bond lengths are close to the sum of their constituent-element atomic radii, i.e., nearly following the Pauling limit, but the lattice constant varies monotonically, having a small deviation from Vegard's law.

Ultrasonic sound velocity measurement techniques can be used to determine the elastic constants of compounds, in which a large, high-quality single-crystal is required. The elastic constants of GaAs and GaP crystals have been measured. The elastic constant c_{11} of $Al_xGa_{1-x}As$ has been determined by the near infrared Brillouin scattering method [4] recently. However, as far as we know, the experimental or theoretical results for $GaAs_{1-x}P_x$ have not been reported.

The electron energy band structure and effective mass of the conduction band in direct-band-gap $GaAs_{1-x}P_x$ alloys ($x < 0.4$) have been measured directly by the optically detected cyclotron resonance or magnetoluminescence technique [5].

In this paper we report the results of the tight-binding studies of $GaAs_{1-x}P_x$ alloys. The local atomic structure and the lattice properties are obtained based on the bond-orbital model (BOM). Using the Slater–Koster Hamiltonian with the simple virtual-crystal approximation (VCA), the trends of the electronic band structure against composition x are calculated. Also the electron effective mass against composition x is estimated based on the $\boldsymbol{k} \cdot \boldsymbol{p}$ theory. The results are compared with experimental and other theoretical results.

The paper is organized as follows: section 2 describes the method used for the present calculation. The results are presented in section 3, followed by a discussion and comparisons with available experiments. A brief summary of our conclusions is contained in section 4.

2. Theoretical formalism

2.1. Bond length relaxation

An approximate estimation of the impurity-host relaxation in zincblende structure semiconductors has been suggested by Baranowski [6]. In tetrahedrally coordinated solids four orthogonal and normalized sp^3 hybrids are chosen in which the electron charge density is the greatest in the direction of the nearest neighbours. In the notation of Harrison [7], the gain in the impurity-host bond energy per bond connected with a distortion Δd ($\Delta d > 0$ outward and $\Delta d < 0$ inward) can be calculated as follows

$$\Delta E_b = \Delta E_b^1 + 3\Delta E_b^2 \tag{1}$$

where ΔE_b^1 and ΔE_b^2 are, respectively, the changes in the energies of the bonds caused by distortion in the nearest- and second-nearest-neighbour atom positions. These are given by

$$\Delta E_b^1 = -2\{[V_2^2(d_0 + \Delta d) + V_3^2]^{1/2} - V_2^2(d_0 + \Delta d)/k|\bar{\varepsilon}_h| \\ -[V_2^2(d_0) + V_3^2]^{1/2} + V_2^2(d_0)/k|\bar{\varepsilon}_h|\} \tag{2}$$

and

$$\Delta E_b^2 = -2\{[V_2'^2(d_0 + \Delta d') + V_3'^2]^{1/2} - V_2'^2(d_0 + \Delta d')/k'|\overline{\varepsilon'}_h| \\ -[V_2'^2(d_0) + V_3'^2]^{1/2} + V_2'^2(d_0)/k'|\overline{\varepsilon'}_h|\} \tag{3}$$

where V_2, V_3 and $k|\bar{\varepsilon}_h|$ refer to the covalent and polar bond energies and the average hybrid energy of the impurity nearest-neighbour bond, respectively; $\Delta d'$ is the change in the bond length between the first- and second-nearest-neighbour. If we hold the second-nearest-neighbours fixed, the following formula can be obtained,

$$\Delta d' = (d_0^2 - 2/3d_0\Delta d + (\Delta d)^2)^{1/2} - d_0. \tag{4}$$

Under the first-order approximation, $\Delta d' = -\Delta d/3$. The terms V_2', V_3' and $k'|\overline{\varepsilon'}_h|$ are the covalent and polar bond energies and average hybrid energy of the host crystal, respectively. Within this approximation, the minimum of the total energy predicates the impurity-host relaxation.

2.2. Elastic constants

Tight-binding theory has been able to obtain approximate but meaningful predictions of the bonding properties of solids. Following Harrison [7], the bond polarity of the compound can be obtained by

$$\alpha_p = \frac{V_3}{(V_2^2 + V_3^2)^{1/2}} \tag{5}$$

where the V_2 is the hybrid covalent energy, which can be approximated in the following way,

$$V_2 = -\eta_\sigma \frac{\hbar^2}{md^2} \tag{6}$$

in which d is the bond length of the compound. The V_3 is the hybrid polar energy, which can be approximated in the following way,

$$V_3 = \tfrac{1}{2}(\varepsilon_h^c - \varepsilon_h^a) \tag{7}$$

where the ε_h^c and ε_h^a are the cation and anion hybrid energy where for sp^3 bonds,

$$\varepsilon_h^c = \tfrac{1}{4}(\varepsilon_S^c + 3\varepsilon_P^c) \qquad \varepsilon_h^a = \tfrac{1}{4}(\varepsilon_S^a + 3\varepsilon_P^a) \tag{8}$$

in which ε_S^c, ε_P^c, ε_S^a, and ε_P^a, are the energies for s and p states for the cation and anion in the solid, respectively. These values could differ somewhat from the corresponding values defined for the free atom; following Harrison [7], we will use free-atom values.

Baranowski [6] made a very simple modification of the overlap interaction on the basis of the idea and method proposed by Harrison [7], and gave the formulae for elastic constants for tetrahedral compounds. The bulk modulus is given by

$$B = \frac{2\sqrt{3}}{3}[V_2^*(1 - \alpha_p^2)^{3/2} + 7.8]\frac{1}{d^5} \tag{9}$$

in which the first term gives the contribution to the bulk modulus of σ bond origin, and $V_2^* \equiv V_2 d^2$, and the second term is the contribution of the π interactions between bonds.

The elastic shear constant $(c_{11} - c_{12})/2$ is given by

$$\frac{c_{11} - c_{12}}{2} = \frac{\sqrt{3}}{4}\left[V_2^*(1 - \alpha_p^2)^{3/2}(1 + \lambda) - \frac{3}{4}(1 - \alpha_p^2)^{1/2}|V_{PP\pi}^*|\right]\frac{1}{d^5} \tag{10}$$

where λ is a dimensionless parameter [6], it takes a constant value of 0.738 and $V_{PP\pi}^* \equiv V_{PP\pi}d^2 = \eta_{PP\pi}\frac{\hbar^2}{m}$, and $V_{PP\pi}$ is the matrix element [7]

Combining equations (9) and (10) and $B = \tfrac{1}{3}(c_{11} + 2c_{12})$, we can obtain the elastic constants

$$c_{11} = \frac{\sqrt{3}}{3}\left[V_2^*(1 - \alpha_p^2)^{3/2}(3 + \lambda) - \frac{3}{4}(1 - \alpha_p^2)^{1/2}|V_{PP\pi}^*| + 2 \times 7.8\right]\frac{1}{d^5} \tag{11}$$

and

$$c_{12} = \frac{\sqrt{3}}{6}\left[V_2^*(1 - \alpha_p^2)^{3/2}(3 - \lambda) + \frac{3}{4}(1 - \alpha_p^2)^{1/2}|V_{PP\pi}^*| + 4 \times 7.8\right]\frac{1}{d^5}. \tag{12}$$

The macroscopic elastic constants B and $(c_{11} - c_{12})/2$, are related to force constants α, β by the equations [8]

$$3B = \frac{\sqrt{3}}{4d}(3\alpha + \beta) - 0.355SC_0 \qquad c_{11} - c_{12} = \frac{\sqrt{3}}{d}\beta + 0.053SC_0 \tag{13}$$

where SC_0 is the Coulomb contribution. The bond stretching force constant α and bond bending force constant β can be obtained by

$$\beta = \frac{d}{\sqrt{3}}[(c_{11} - c_{12}) - 0.053SC_0] \qquad \alpha = \frac{4d}{\sqrt{3}}\left[B + 0.355\frac{SC_0}{3}\right] - \frac{1}{3}\beta. \tag{14}$$

The elastic stiffness constant c_{44} is given by [8]

$$c_{44} = \frac{\sqrt{3}}{4d}(\alpha + \beta) - 0.136SC_0 - c\xi^2 \tag{15}$$

where

$$c = \frac{\sqrt{3}}{4d}(\alpha + \beta) - 0.266SC_0 \tag{16}$$

and

$$\xi = c^{-1}\left[\frac{\sqrt{3}}{4d}(\alpha - \beta) - 0.294SC_0\right]. \tag{17}$$

2.3. Band structure

The energy band structure of $GaAs_{1-x}P_x$ is described by use of the tight-binding Slater–Koster Hamiltonian of binary in the VCA. Following Harrison [7], the weighted average tight-binding parameter p_i for the alloy crystal including the on-site matrix elements and the second-neighbour parameters are linearly interpolated as a function of x, i.e.,

$$p_i(GaAs_{1-x}P_x) = (1 - x) \cdot p_i(GaAs) + x \cdot p_i(GaP). \tag{18}$$

Considering the dependence of p_i on the bond length in $GaAs_xP_{1-x}$, the nearest-neighbour off-diagonal matrix elements can be obtained by

$$d^2(x) \cdot p_i(GaAs_{1-x}P_x) = d_{GaAs}^2(x) \cdot (1 - x) \cdot p_i(GaAs) + d_{GaP}^2(x) \cdot x \cdot p_i(GaP) \tag{19}$$

where $d_{GaAs}(x)$, $d_{GaP}(x)$, and $d(x)$ are the bond lengths of GaAs, GaP and average bond length in $GaAs_{1-x}P_x$, respectively, and

$$d(x) = (1 - x) \cdot d_{GaAs}(x) + x \cdot d_{GaP}(x). \tag{20}$$

These assumptions leave the symmetry of the alloy unchanged, i.e., the tetrahedral structure remains. Since there is little bowing in the fundamental band edge of this alloy, this approximation is known to be quite reasonable.

2.4. Effective mass

The $\boldsymbol{k} \cdot \boldsymbol{p}$ perturbation theory gives the expressions of energies and wave functions near a semiconductor band extremum. The effective mass is inversely proportional to the energy band curvature. For a conduction electron at $\boldsymbol{k} = 0$ in a cubic semiconductor, the effective mass is expressed by [9]

$$\frac{m_0}{m^*} - 1 = \frac{P^2}{3}\left(\frac{2}{E_0} + \frac{1}{E_0 + \Delta_0}\right) - \frac{P'^2}{3}\left(\frac{2}{E(\Gamma_8^c) - E_0} + \frac{1}{E(\Gamma_7^c) - E_0}\right) + C \tag{21}$$

in which E_0 is the $\Gamma_8^v - \Gamma_6^c$ gap, Δ_0 the valence band spin-orbit splitting. P is the momentum matrix element connecting the p-type valence band with the s-type conduction band, and P' is the momentum matrix element connecting the s-type conduction band with next higher-lying p-type conduction bands. C is a small correction for all higher-lying bands. Because the conduction and valence band wave function differ from GaAs to GaP, in order to calculate the effective mass of $GaAs_{1-x}P_x$, it must be expected that P and/or P' will also vary with P composition x.

3. Results and discussion

In this section we present the results of our tight-binding calculations for the bond lengths in GaAs$_{1-x}$P$_x$ alloys and the trends in elastic constants, the electronic band structure and effective mass as the function of composition x and compare them with the available experimental results.

3.1. Bond lengths

The bond lengths around the impurity for two systems GaAs:P and GaP:As are obtained based on BOM calculation. The lattice relaxations (Δd) are -0.066 and 0.065 Å, respectively. The bond lengths of GaAs and GaP in the dilute limit are 2.424 and 2.380 Å. Martins and Zunger [10] have recently calculated the bond lengths in crystalline GaAs$_{1-x}$P$_x$ alloy by a valence force-field (VFF) model. The bond lengths of GaAs and GaP in the dilute limit are 2.414 and 2.387 Å. The dimensionless relaxation parameters for GaAs and GaP bonds are about 0.62 and 0.68. A serious discrepancy exists between the VFF calculation and the EXAFS analysis (0.82) [3]. According to our calculation, the values for GaAs:P and GaP:As are about 0.76 and 0.75, respectively. Although the difference between our results and EXAFS experimental results is also significant, our results are closer to the results obtained by the EXAFS experiment [3].

It is clear from EXAFS experiment that the relationship between the bond length $d_{\text{GaAs}}(x)$ and $d_{\text{GaP}}(x)$ and the composition is nearly linear. So our model for the dilute alloy can be extended to the whole range of composition by a linear interpolation of the data of the end-point materials. The results of our BOM of the GaAs and GaP bond lengths in GaAs$_{1-x}$P$_x$ alloys are shown in figure 1 along with the VFF results[10] and experimental results obtained by the EXAFS technique [3]. The bond lengths of GaAs are in the range of 2.424 and 2.446 Å, while the bond length of GaP is in the range of 2.359 and 2.380 Å. All of the largest relative deviations of bond lengths in alloys from the bond lengths in two compounds are about 0.9%. Therefore, the GaAs and GaP bond lengths in alloys tend to maintain their respective lengths: nearly 2.446 Å for the GaAs bond and 2.359 Å for the GaP bond.

The average bond length of GaAs$_{1-x}$P$_x$ can be obtained by the weighted average bond length over $d_{\text{GaAs}}(x)$ and $d_{\text{GaP}}(x)$. The experimental result (circles) and our result (dashed line) are shown in figure 1. We find that the $d(x)$ varies monotonically, nearly follows Vegard's law. Our result has a very small negative deviation -0.01% at $x = 0.5$ from Vegard's law, for the experimental result it is about -0.06%. The bond lengths $d_{\text{GaAs}}(x)$, $d_{\text{GaP}}(x)$ and $d(x)$ will be used to calculate the elastic constants and electronic band structure.

3.2. Elastic constants

To the best of our knowledge, the elastic constants of GaAs$_{1-x}$P$_x$ alloys have never been measured or calculated. Here we present the results of the BOM calculation for the polarity α_p, bulk modulus B, elastic shear constants c_{11}, c_{12} and c_{44}, bond-stretching force constant α and bond-bending force constant β, Young's modulus and sound velocities of GaAs$_{1-x}$P$_x$ alloys.

From equations (9)–(12), we know that the elastic constants are dependent on two parameters, i.e., bond length d and bond polarity α_p. Using the virtual-crystal approximation (VCA), the free-atom energies for s and p states for the anion, i.e., ε_S^a, ε_P^a can be obtained by the linear interpolation $\varepsilon_S^a = (1 - x)\varepsilon_S^{\text{As}} + x\varepsilon_S^{\text{P}}$, $\varepsilon_P^a = (1 - x)\varepsilon_P^{\text{As}} + x\varepsilon_P^{\text{P}}$. Take the
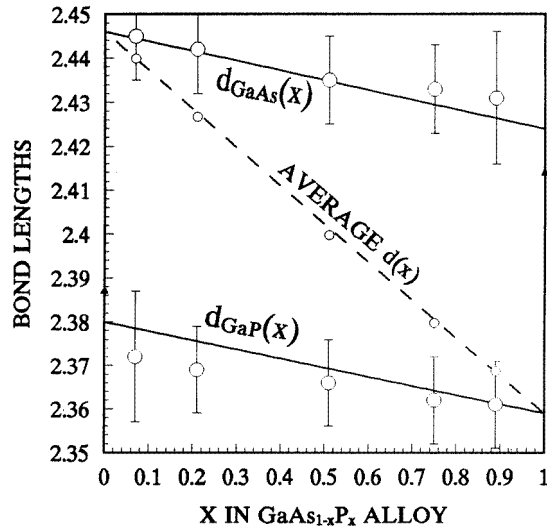
Figure 1. GaAs and GaP bond lengths (in Å), as a function of P concentration x in $GaAs_{1-x}P_x$ alloys. The solid lines present our BOM results. The circles and error bars present the EXAFS measuremental results [3]. The dashed line and circles are the average of our results and experimental results, respectively. The triangles are the VFF results [10].

average bond length $d(x)$ as that of $GaAs_{1-x}P_x$ alloys, the polarities of $GaAs_{1-x}P_x$ alloys can be obtained. Then the bulk modulus B, elastic shear constants of $GaAs_{1-x}P_x$ alloys can be obtained. The results for GaAs, GaP and $GaAs_{1-x}P_x$ alloys are given in table 1, and compared with the available experimental results.

As far as we know, many works have studied the polarities of GaAs and GaP, however, all of these results are appreciably different. So the determination of polarity will be very important to elastic constants. Our results are in good agreement with the results of [11] calculated from experiments.

It is clear from table 1 that the bulk modulus and elastic shear constants for GaAs and GaP obtained by BOM are in good agreement with the experimental results [12–14]. The results of calculated elastic constants c_{11}, c_{12} and c_{44} for $GaAs_{1-x}P_x$ alloys are given by solid lines in figure 2. They have small negative deviations from the linear average of that of GaAs and GaP compounds. It shows an approximate linear increase with increasing P composition x.

It is clear from equations (9), (11) and (12) that elastic constants tend to decrease with increasing bond length and polarity of the valence bonds (because $V_2^*(3+\lambda) \gg \frac{3}{4}|V_{PP\pi}^*|$), but the relations look nonlinear. How is it that the results show a approximate linear increase with increasing P composition x? In fact, for $GaAs_{1-x}P_x$, because the difference in bond lengths between GaAs and GaP is small (-3.557%), we have $[1 + 5 \times 0.03557]/[(1 - 0.03557)^{-5}] \approx 98.28\%$, then we have $(1 - 0.03557x)^{-5} \approx 1 + 5 \times 0.03557x$, and so it shows an approximation linear increase with decreasing bond length. The relative change in elastic constants c_{11}, c_{12} and bulk modulus B caused by the variation of bond length is about 19.85% from $x = 0$ to 1. Because the change in polarity from GaAs to GaP is very small (-0.6%), we have $\{1 - [0.319(1 - 0.006x)]^2\}^{3/2} \approx 1 - \frac{3}{2} \times 0.319^2(1 - 2 \times 0.006x)$, and $\{1 - [0.319(1 - 0.006x)]^2\}^{1/2} \approx 1 - \frac{1}{2} \times 0.319^2(1 - 2 \times 0.006x)$. So they show an approximate

Table 1. Bulk material parameters for GaAs, GaP, and the alloy GaAs$_{1-x}$P$_x$. The average bond length d is in Å. The crystal density ρ is in g cm^{-3}. The bulk modulus B, Young's modulus and elastic stiffness constants are in 10^{11}dyn cm^{-2}, force constant α and β are in units of 10^3dyn cm^{-1}. The sound velocities are in units of 10^5 cm s-1.

	GaAs	GaP	GaAs$_{1-x}$P$_x$
d	2.446	2.359	$2.446\times(1-0.03557x)$
ρ	5.332	4.146	$5.332\times(1-0.2222x)$
α_p	0.319	0.317	$0.319\times(1-0.006x)$
	0.30[a]	0.31[a]	
B	7.63	9.16	$7.63\times(1+0.177x+0.023x^2)$
	7.69[b]	8.94[c]	
c_{11}	12.37	14.85	$12.37\times(1+0.177x+0.023x^2)$
	12.11[b]	14.39[d]	
c_{12}	5.26	6.32	$5.26\times(1+0.177x+0.023x^2)$
	5.48[b]	6.52[d]	
c_{44}	5.97	7.22	$5.97\times(1+0.185x+0.023x^2)$
	6.04[b]	7.14[d]	
α	41.74	48.59	$41.74\times(1+0.149x+0.015x^2)$
	41.25[e]	44.50[e]	
β	9.83	11.35	$9.83\times(1+0.139x+0.016x^2)$
	9.25[e]	10.69[e]	
ν	0.2984	0.2983	$0.2984\times(1-0.0003x)$
E_{100}	9.233	11.09	$9.233\times(1+0.177x+0.023x^2)$
		10.311[f]	
E_{110}	12.53	15.09	$12.53\times(1+0.181x+0.023x^2)$
		14.614[f]	
E_{111}	14.22	17.15	$14.22\times(1+0.183x+0.023x^2)$
v_1	4.821	5.987	$4.821\times(1+0.195x+0.046x^2)$
	4.727[g]	5.847[h]	
v_2	3.350	4.173	$3.350\times(1+0.199x+0.046x^2)$
	3.344[g]	4.131[h]	
v_3	5.271	6.554	$5.271\times(1+0.197x+0.046x^2)$
	5.234[g]		
v_4	3.350	4.173	$3.350\times(1+0.199x+0.046x^2)$
	3.368[b]		
v_5	2.584	3.209	$2.584\times(1+0.196x+0.046x^2)$
	2.500[b]		
v_6	5.413	6.732	$5.413\times(1+0.197x+0.046x^2)$
	5.446[b]	6.648[h]	
v_7	2.862	3.560	$2.862\times(1+0.197x+0.046x^2)$
	2.821[b]	3.466[h]	

[a] Reference [11] [b] Reference [12] [c] Reference [13]
[d] Reference [14] [e] Reference [15] [f] Reference [16]
[g] Reference [17] [h] Reference [18]

linear increase with decreasing bond polarity. According to the above arguments, we find that the elastic constants of GaAs$_{1-x}$P$_x$ increase approximately linearly with increasing P composition. From our results in table 1, apparently the changes in elastic constants c_{11}, c_{12} and bulk modulus B from GaAs to GaP are about 20%. Because of the change caused by the variation of bond length is about 19.85% from GaAs to GaP, so the change caused by the variation of bond polarity is only 0.15% from GaAs to GaP. Therefore, the increase is dominated by the change in bond length in GaAs$_{1-x}$P$_x$.

Using the data of $S = 0.441$ and $C_0 = 6.418$ for GaAs and $S = 0.514$ and $C_0 = 7.430$

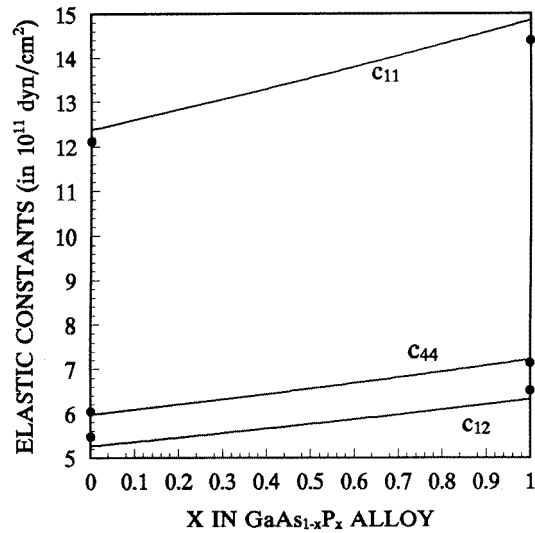**Figure 2.** Elastic constants c_{11}, c_{12} and c_{44} (in 10^{11} dyn cm^{-2}) of GaAs$_{1-x}$P$_x$ alloys as functions of P composition x. Solid circles are measured results [12,14]. The solid lines present our BOM result.

for GaP [8] from equation (14) we find that the Coulomb contribution to the bond-stretching force constant α and bond-bending force constant β is rather small, it can be dismissed. However, the inclusion of the Coulomb contribution will make the results of α, β and c_{44} agree much better with experiments [15]. Because the difference of Coulomb contribution for GaAs and GaP is very small, the S and C_0 of GaAs$_{1-x}$P$_x$ alloys can be obtained by linear interpolation. The calculated results for α and β and c_{44} from equation (14) are given in table 1, and compared with the available results [15]. Then we find that the force constants α and β, and elastic constant c_{44} are also approximate linearly increasing with increasing P composition and are dominated by the change in bond length in GaAs$_{1-x}$P$_x$.

In cubic crystals several relations hold between the parameters characterizing the lattice properties. According to the relations, the Young's modulus E_{100}, E_{110} and E_{111}, Poisson's ratio ν, and sound velocities v_i ($i = 1, \ldots, 7$) can be obtained. The results are also given in table 1. It is clear that from table 1 our results are in good agreement with the experimental results [12,16–18]. The Young's modulus and sound velocities monotonically increase with increasing P composition. The trends of Young's modulus E_{100}, E_{110} and E_{111} are nearly the same and are the same as the results of elastic constant c_{11}, c_{12} and c_{44} and bulk modulus B. The trends of velocities are also nearly the same, as can be seen from table 1 and figure 3. The Poisson's ratio is nearly the same for GaAs and GaP, because it is independent of bond length.

3.3. Electronic band structure

Here we use the Hamiltonian of Talwar and Ting of [19] and the parameters given there for the compounds GaAs and GaP. We proceed to obtain the alloy Hamiltonian using the VCA, then the band structure can be obtained by the diagonalization method.

The variation of the Γ and X symmetry-points energies (minima of the conduction band) with the composition x are given in figure 4. Our theoretical curves (solid lines) are in good
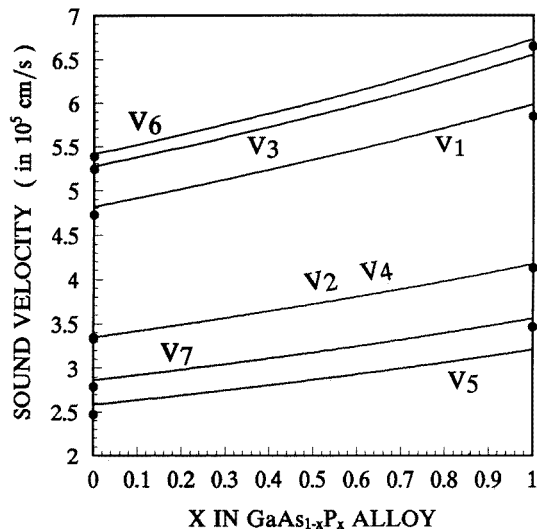
Figure 3. Sound velocities v_i, ($i = 1, \ldots, 7$) (in 10^5 cm s^{-1}) of GaAs$_{1-x}$P$_x$ alloys as functions of P composition x. Solid circles are measured results [12,17,18]. The solid lines present our result.
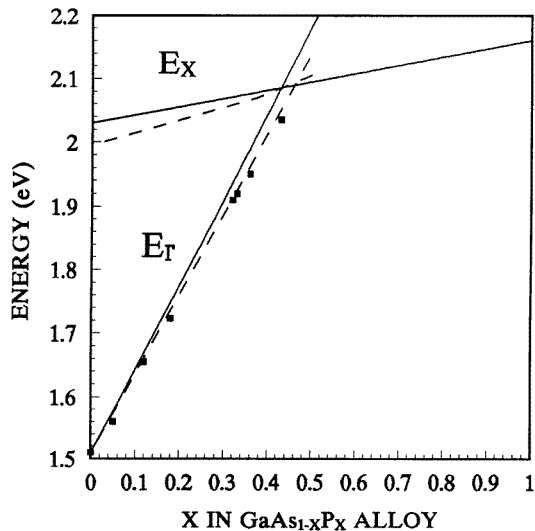

Figure 4. The conduction-band edge as function of P composition x, where the zero of energy is taken to be the tops of the valence-band edge for all x. The crossover point occurs at $x = 0.43$. The solid lines present our results. The solid squares and dashed lines present the experimental results [5].

agreement with the experimental ones (dashed lines [5]). Our values for the energies of the band minima are $E_\Gamma = 1.51 + 1.33x + 0.043x^2$ and $E_X = 2.03 + 0.137x - 0.005x^2$. They are also almost the same as the experimental results [20]: $E_\Gamma = 1.514 + 1.174x + 0.186x^2$ and $E_X = 1.977 + 0.144x + 0.211x^2$ (for $T = 77K$). We find that the crossover point from

a direct gap at $\Gamma(0,0,0)$ to $X(1,0,0)\frac{2\pi}{a}$ occurs at $x = 0.43$. This is in good agreement with experimental results [5], $x = 0.45$.

In the direct-band-gap $GaAs_{1-x}P_x$, the x dependence of E_0 can be given by: $E_0 = 1.51 + 1.35x + 0.015x^2$ (eV). For the higher conduction band the result is $E(\Gamma_5^c) = 4.55 + 0.65x + 0.035x^2$ (eV).

In addition, when the bond lengths of $d_{GaAs}(x)$ and $d_{GaP}(x)$ in equations (17) and (18) are taken as the bond lengths d_{GaAs} and d_{GaP} of compounds GaAs and GaP at same time, for the direct-band-gap $GaAs_{1-x}P_x$, the x dependence of E_0 can be given by: $E_0 = 1.51 + 1.32x + 0.052x^2$ (eV) and the higher conduction band is $E(\Gamma_5^c) = 4.55 + 0.65x + 0.045x^2$ (eV). So although the change in bond lengths has an effect on the structure of the energy band, but the effect is very small.

3.4. Effective mass

In the direct-band-gap $GaAs_{1-x}P_x$ alloys, we assume a linear variation of spin–orbit splitting Δ_0 and Δ_0' with x, and $\Delta_0 = 0.341$–$0.261x$ (eV), $\Delta_0' = 0.171$–$0.091x$ (eV) [21,22]. We use the relationship: $E(\Gamma_7^c) = E(\Gamma_5^c) - \Delta_0'/2$ and $E(\Gamma_8^c) = E(\Gamma_5^c) + \Delta_0'/2$. The interband matrix element P^2 is slightly dependent on x, and is taken to be linear function of x [5]: $P^2 = 28.9 + 2.5x$ (eV). $P'^2 = 6$ eV and $C = -2$ are supposed to be constants in $GaAs_{1-x}P_x$ alloys.
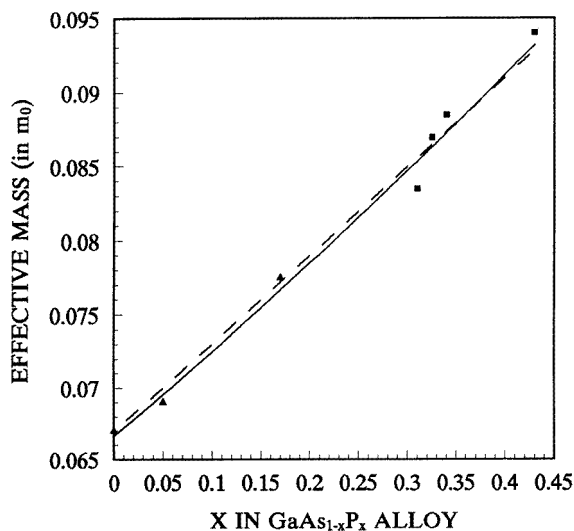

Figure 5. Values for effective mass in $GaAs_{1-x}P_x$ alloys. Triangles mark ODCR and squares present magnetoluminescence results [5]. The dashed line is the result of the linear fit to the experimental points. The solid line is our $\mathbf{k} \cdot \mathbf{p}$ theory result.

The calculated effective mass m^* values for the investigated alloy composition range are plotted in figure 5 (solid line). We note that the agreement with the mass dependence obtained from the optically detected cyclotron resonance experiments and the diamagnetic shift (triangles and squares) is very satisfactory. In figure 5 the dashed line is the best linear fit $m^* = 0.067 + 0.06x$ (m_0) obtained from the experimental data. Our result can be given by $m^* = 0.0664 + 0.0586x + 0.0086x^2$ (m_0).

4. Conclusions

The tight-binding bond orbital model is used to predict the GaAs and GaP bond lengths in GaAs$_{1-x}$P$_x$ alloys. The results are compared with the other theoretical and the experimental results, and are in good agreement with EXAFS experiment. The average bond length varies monotonically, has a small, negative deviation from Vegard's law. The GaAs and GaP lengths are close to Pauling limit, but are composition dependent.

The calculated bond polarities and the bulk modulus, elastic constants, force constants, Young's modulus, Poisson's ratio and sound velocities of GaAs and GaP are in good agreement with existing experimental data. All of the results of GaAs$_{1-x}$P$_x$ are predicated. It is found that the bulk modulus, elastic constants, force constants, Young's modulus, Poisson's ratio and sound velocities monotonically increase with increasing P composition (it has a small negative deviation from the linear average, i.e., the bowing parameters are greater than zero) and the increase is dominated by the change in average bond length.

The electronic band structure of GaAs$_{1-x}$P$_x$ is obtained. We find that the crossover from direct- to indirect-band-gap at $x = 0.43$, and the dependencies of the direct- and indirect-gap on x are nearly linear. The results of the direct-band-gap energy are in good agreement with the photoluminescence measurement data. The effective electron mass associated with the conduction band minimum in direct-band-gap GaAs$_{1-x}$P$_x$ alloy obtained by the $\boldsymbol{k} \cdot \boldsymbol{p}$ theory is in good agreement with the optically detected cyclotron resonance and magnetoluminescence experimental results.

References

[1] Pauling L 1967 *The Nature of the Chemical Bond* (New York: Cornell University)
[2] Vegard L 1921 *Z. Phys.* **5** 17
[3] Wu Zhonghua, Lu Kunquan, Wang Yuren, Dong Jun, Li Hefeng and Li Chenxi 1993 *Phys. Rev.* B **48** 8694
[4] Krieger M, Sigg H and Reinhart F K 1993 *Solid State Commun.* **88** 267
[5] Wetzel C, Meyer B K and Omling P 1993 *Phys. Rev.* B **47** 15588
[6] Baranowski J M 1984 *J. Phys. C: Solid State Phys.* **17** 6287
[7] Harrison W A, 1980 *Electronic Structure and the Properties of Solid,* (New York: Freeman)
[8] Martin R M 1970 *Phys. Rev.* B **1** 4005
[9] Hermann C and Weisbuch C 1977 *Phys. Rev.* B **15** 823
[10] Martins J L and Zunger A 1984 *Phys. Rev.* B **30** 6217
[11] Falter C, Ludwig W, Selmke M and Zierau W 1984 *Phys. Lett.* **105A** 139
[12] Cottam R I, Saunders G A 1973 *J. Phys. C: Solid State Phys.* **6** 2105
[13] Muramatsu S and Kitamura M 1993 *J. Appl. Phys.* **73** 4270
[14] Boyle W F and Sladek R J 1975 *Phys. Rev.* B **11** 2933
[15] Keating P N 1966 *Phys. Rev.* **145** 637
[16] Gyrbu I N 1978 *Sov. Phys. Solid State (Engl. Transl.)* **20** 2006
[17] McSkimin H J, Jayaraman A and Andreatch P 1967 *J. Appl. Phys.* **38** 2362
[18] Weil R and Groves W O 1968 *J. Appl. Phys.* **39** 4049
[19] Talwar D N and Ting C S 1982 *Phys. Rev.* B **25** 2660
[20] Kleiman G G 1977 *Phys. Rev.* B **15** 802
[21] Stokowski S E and Sell D D 1972 *Phys. Rev.* B **5** 1636
[22] Aspnes D E and Studna A A 1973 *Phys. Rev.* B **7** 4605